Outage Analysis of Downlink NOMA Full-Duplex Relay Networks with RF Energy Harvesting over Nakagami-m Fading Channel

Nguyen Trung Tan[1], Tran Manh Hoang[1], Ba Cao Nguyen[1], and Le The Dung[2(✉)]

[1] Department of Radio, Le Quy Don Technical University, Hanoi, Vietnam
trungtan68@gmail.com, tranmanhhoang@tcu.edu.vn, bacao.sqtt@gmail.com
[2] Department of Radio, Chungbuk National University, Cheongju, Korea
dung.t.le@ieee.org

Abstract. In this paper, we propose and analyze a downlink non-orthogonal multiple access (NOMA) relay system with full-duplex transition model and decode and-forward (DF) scheme. We assume that the source and the destinations node have fixed power, whereas relay nodes have constrained energies and should harvest radio frequency (RF) energy from the source for operation power. The full duplex is assumed and the outage performance of this system is analyzed over the Nakagami-m fading channel with imperfect channel state information (CSI). The closed-form of outage probabilities are derived and evaluated in several scenarios. Moreover, the optimal power allocation coefficients which lead to the minimal outage probability while keeping the fairness in outage performance of end users are discussed. The analytical results are verified by the Monte-Carlo simulation.

Keywords: Non-orthogonal multiple access (NOMA)
Channel state information (CSI) · Energy harvesting (EH)
Radio frequency (RF) · Successive interference cancellation (SIC)
Full-duplex relay system · Decode and forward scheme

1 Introduction

The Non-orthogonal multiple access (NOMA) has been a promising multiple access technique for the fifth generation (5G) mobile networks due to its superior spectral efficiency [1]. The key idea of NOMA is to employ the power domain where different users are served at different power levels [2]. The studying for NOMA has also been applied to cooperative relay systems [3, 4]. In [3], the relay node was assumed to possess a buffer, the authors proposed an adaptive transmission scheme in which the system adaptively chooses its working mode in each time slot.

The authors of [4] proposed and investigated a dual-hop cooperative relay scheme using NOMA, where two sources communicate with their corresponding destinations in parallel over the same frequency band and a common relay. However, the power

H. Fujita et al. (Eds.): ICERA 2018, LNNS 63, pp. 477–487, 2019.
https://doi.org/10.1007/978-3-030-04792-4_62

control for multiple access uplink was not considered. In addition, harvesting energy from the ambient environment has become a promising solution for energy-constrained electronic devices, which are conventionally supported by limited power sources such as battery [5–7].

In some special applications charging the battery is too expensive or even impossible, e.g. sensors in toxic environment or in body area networks. Moreover, some natural energy sources such as solar and wind, and radio frequency (RF) can be also utilized as effective sources for energy harvesting (EH). Compared with other kinds of energy sources, the RF-based energy harvesting, also called the wireless energy transfer, has some advantages [8]. Therefore, the utilizing RF-EH technique with the NOMA scheme helps to prolong the lifetime and improves the spectral utilizing efficiency of the energy-constrained multi-user wireless relay networks [9–11].

A new cooperative multiple-input single-output (MISO) with SWIPT of NOMA system, where the user having a strong channel condition acts as an EH relay to help the user with a weak channel condition is proposed in [12]. To maximize the data rate of the user with the strong channel condition, while satisfying the QoS requirements of the user suffering from a weak channel condition, the authors proposed the optimizing power-splitting (PS) and beam forming vectors based on solving the global optimality problem. Furthermore, the cooperative spectrum sharing in the EH-NOMA network with the best secondary user selection was proposed in [13]. This network system is investigated in several scenarios for different application purposes.

Most of the previous works for NOMA relay system are considered with Rayleigh fading and the perfect channel state information (CSI). However, due to channel estimation errors, this assumption is unrealistic. In addition, the channel model of Nakagami-m distribution is more general than Rayleigh distribution models. Motivated by these observations, in this paper, we propose a different cooperative decode-and-forward relay scheme where a source transmits modulation superposition to two users via an assistant relay harvesting energy from the RF. Based on the channel gain from the relay node to the destination's node, the relay performs power reallocation for two users. Furthermore, we consider the full-duplex relay model for forwarding signals to two destinations in condition the channel distribution of Nakagami-m with channel estimation error. The results of this work consist of: (1) Detection the outage probability expressions for both destinations with respect to NOMA scheme; (2) Investigation of the impact of the strength loop interference and channel estimation error; (3) Derivation of power allocation for minimizing the outage probability.

Our proposed system can be applied in surveillance sensor networks for disaster detection or Internet of Things (IoT), where installing fixed power lines or frequency replacing the batteries for a large number of nodes is not convenient. In addition, its advantages such as low energy cost, reducing greenhouse effect, and prolonging time life are useful for the future 5G networks.

The rest of the paper is organized as follows. The channel model is described in Sect. 2. The system is analyzed in Sect. 3 and the calculation result is represented in Sect. 4. Finally, the Sect. 5 concludes the paper.

2 System Model

The system model of a NOMA downlink relay network investigated in this paper is shown in Fig. 1. According to this model, a source (S) wants to send the messages to two destinations (D1) and (D2) simultaneously with the help of a decode-and-forward (DF) relay (R). It is assumed that S, D1, and D2 have constant power supply but the relay node has constrained power supply and can harvest energy from the RF (Radio Frequency) transmitted by the S. According to the principle of NOMA, the source combines signals for D_1 and D_2, which are respectively denoted by x_1 and x_2, to a superposition signal with different power lever and transmits to the relay. The relay decodes, regenerates the superposition signal following NOMA method and then forwards to the destinations. At D_1 and $D\text{-}_2$, the desired signal is decoded following successive interference cancellation (SIC) algorithm. The channels between of two terminals are subject to block and flat Rayleigh fading, which means channel coefficients keep constant during the transmission block T and vary from block to block.

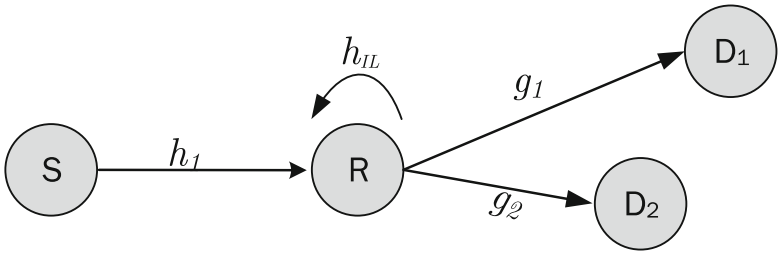

Fig. 1. System model.

In order to allocate transmission power for D_1 and D_2, the source requires the CSI as well as the channel gains S → R and R → D_i. It should be noticed that obtaining the perfect CSI of wireless network is extremely difficult due to the channel estimation error. In practice, the CSI can be obtained by pilot-assisted channel training or with the help of a suitable feedback mechanism[1]. The feedback delay and estimation error are the main reasons of imperfect CSI. This paper, we only consider imperfect CSI due to channel estimation error. Thus, the channel estimation process is modelled as [14]

$$h_1 = \hat{h}_1 + \varepsilon_h, \tag{1}$$

$$g_i = \hat{g}_i + \varepsilon_i, i = \{1, 2\}, \tag{2}$$

[1] Pilot symbols are periodically inserted into the data symbols at the transmitter so that the channel-induced envelope fluctuation fading amplitude and phase, which can be extracted and interpolated at the channel estimation stage.

where $\hat{h}_1$ and $\hat{g}_i$ are respectively the estimated version of h_1 and g_i the $\varepsilon_i \sim CN(0, \sigma^2_{\varepsilon_i})$ is the channel estimation error, which can be considered as a Gaussian distribution [15]. In addition, $\hat{\Omega}_A = \Omega_A - \sigma^2_{\varepsilon_A}$ with $A \in \{\mathrm{SR}, \mathrm{RD}_1, \mathrm{RD}_2\}$ are channel gains of the $\hat{h}_1$ and $\hat{g}_i$. The $\hat{h}_1$, $\hat{g}_i$ are statistically independent of ε_i and ε_h. We let $0 \le \rho_A \le 1$ are the correlation coefficients of channel estimation error and channel estimation perfect. Because of $\sigma^2_{\varepsilon_A} = \rho_A \Omega_A$, we have variable of estimation channel error as $\hat{\Omega}_A = (1 - \rho_A)\Omega_A$.

As shown in Fig. 1, the complex channel coefficient between S and R is denoted as $h_1 \sim CN(0, \hat{\Omega}_{\mathrm{SR}})$. The complex channel coefficient between R and D_i, is $g_i \sim CN(0, \hat{\Omega}_{\mathrm{RD_i}})$, where $i = \{1, 2\}$. The additive white Gaussian noise (AWGN) at R, D_1 and D_2 is denoted as $w_A \sim CN\left(0, \sigma^2_R\right)$. Without loss of generality, we assume that the order of users' channel gains is $|g_1|^2 < |g_2|^2$. Let T denote the block time of an entire communication period in which the information is transmitted from S to $\mathrm{D_i}$. At every T period, the first αT amount of time is used for harvesting energy at the relay node, while the remaining $(1 - \alpha)T$ amount of time is used for transmitting and receiving information, where α denotes the fraction of the block time, $0 \le \alpha \le 1$. Hence, the harvested energy of the relay node in αT amount of time is expressed as [12].

$$E_h = \frac{\eta \alpha T P_{\mathrm{S}}}{\sigma^2_R} |h_1|^2, \tag{3}$$

where η is the energy conversion efficiency coefficient whose value varies from 0 to 1, and P_{S} is the average transmitted power of the source. The energy conversion efficiency coefficient depends on the harvesting electric circuitry and it is often presented as percentages. Compared to the power used for signal transmission, the processing power required by the transmit/receive circuitry at the relay is extremely smaller. Therefore, it is generally negligible, and then the harvested power is assumed to be consumed by the relays for forwarding signals to all users $\mathrm{D_i}$. From (3), the transmission power of the relay, P_{R}, is given by

$$P_{\mathrm{R}} = \frac{E_h}{1 - \alpha} = \frac{\alpha \eta P_{\mathrm{S}} |h_1|^2}{(1 - \alpha)\sigma^2_R}. \tag{4}$$

Since the signal transmitted by the source is superimposed, the received signal at the relay is given by

$$y_{\mathrm{R}} = h_1(\sqrt{a_1 P_{\mathrm{S}}} x_1 + \sqrt{a_2 P_{\mathrm{S}}} x_2) + \sqrt{P_{\mathrm{R}} \kappa} h_{LI} x_{\mathrm{R}} + w_{\mathrm{R}}, \tag{5}$$

where the h_{LI} denotes the loopback interference channel from the transmit antenna to the receive antenna at the relay. Without loss of generality, it follows Rayleigh distribution. The κ is factor index for self-interference-cancellation at the relay node. According to the principle of SIC, firstly the relay decodes the signal x_1 while considering the signal x_2 as noise, and then removes the signal x_1 from the received signal

and decode the signal x_2. Consequently, from (5) we have the instantaneous signal-interference-noise-ratios (SINRs) of S $\rightarrow$ R link as

$$\gamma_{\mathrm{R}}^{x_1} = \frac{a_1 P_{\mathrm{S}} |h_1|^2}{a_2 P_{\mathrm{S}} |h_1|^2 + P_{\mathrm{R}} \kappa |h_{LI}|^2 + \sigma_{\mathrm{R}}^2}, \quad \gamma_{\mathrm{R}}^{x_2} = \frac{a_2 P_{\mathrm{S}} |h_1|^2}{P_{\mathrm{R}} \kappa |h_{LI}|^2 + \sigma_{\mathrm{D_i}}^2}. \tag{6}$$

where $\gamma_{\mathrm{R}}^{x_1}$ and $\gamma_{\mathrm{R}}^{x_2}$ are respectively the SINRs of signals x_1 and x_2 at the relay.

Because of application of full duplex DF protocol, the relay decodes the original signal and then forwards the regenerated signal to the destinations. Thus, the received signal at $\mathrm{D_i}$ can be expressed as

$$y_{\mathrm{D_i}} = g_i(\sqrt{a_1 P_{\mathrm{R}} x_1} + \sqrt{a_2 P_{\mathrm{R}}} x_2) + w_{\mathrm{D_i}}, \tag{7}$$

and the SINR, SNR of the R $\rightarrow$ $\mathrm{D_1}$ and R $\rightarrow$ $\mathrm{D_2}$ links are described as

$$\gamma_{\mathrm{D_1}}^{x_1} = \frac{a_1 P_{\mathrm{R}} |g_1|^2}{a_2 P_{\mathrm{R}} |g_1|^2 + \sigma_{\mathrm{R}}^2}, \quad \gamma_{\mathrm{D_2}}^{x_1 \rightarrow \mathrm{D_2}} = \frac{a_1 P_{\mathrm{R}} |g_2|^2}{a_2 P_{\mathrm{R}} |g_2|^2 + \sigma_{\mathrm{D_2}}^2}, \quad \gamma_{\mathrm{D_2}}^{x_2} = \frac{a_2 P_{\mathrm{R}} |g_2|^2}{\sigma_{\mathrm{D_2}}^2}, \tag{8}$$

where $\gamma_{\mathrm{D_1}}^{x_1}$ and $\gamma_{\mathrm{D_2}}^{x_1 \rightarrow \mathrm{D_2}}$ are respectively the SINR of signal x_1 at $\mathrm{D_1}$ and $\mathrm{D_2}$, while $\gamma_{\mathrm{D_2}}^{x_2}$ is the SNR of signal x_2 at $\mathrm{D_2}$.

3 Outage Analysis

In this section, we derive a closed-form expression of outage probability at each destination. The target transmission rate of x_1 and x_2 is denoted by $r_i, \quad i = 1, 2$. When the instantaneous end-to-end capacity is less than the target transmission rate, the outage event happens. It is equivalent to the probability which the SINR/SNR of x_1 or x_2 falls below a certain threshold, $\gamma_{\mathrm{th_i}} = 2^{\frac{r_i}{1-\alpha}} - 1$.

The probability which the x_1 is not able to be decoded at the relay or the $\mathrm{D_1}$ is represented by

$$\mathrm{OPD_1} = 1 - \Pr(\gamma_{\mathrm{R}}^{x_1} > \gamma_{\mathrm{th_1}}, \gamma_{\mathrm{D_1}}^{x_1} > \gamma_{\mathrm{th_1}}). \tag{9}$$

On the other hand, to successfully decode x_2 at the relay, the SIC of x_1 and the decode of x_2 at the relay should be successfully. Similarly, to successfully decode x_2 at the $\mathrm{D_2}$, the SIC of x_1 and the decode of x_2 at the $\mathrm{D_2}$ should be successfully. Therefore, the outage probability of the $\mathrm{D_2}$ can be described as follows.

$$\mathrm{OPD_2} = 1 - \Pr\begin{pmatrix} \gamma_{\mathrm{R}}^{x_1} > \gamma_{\mathrm{th_1}}, \gamma_{\mathrm{R}}^{x_2} > \gamma_{\mathrm{th_2}}, \\ \gamma_{\mathrm{D_2}}^{x_1 \rightarrow \mathrm{D_2}} > \gamma_{\mathrm{th_1}}, \gamma_{\mathrm{D_2}}^{x_2} > \gamma_{\mathrm{th_2}} \end{pmatrix}. \tag{10}$$

Recall that the probability density functions (PDFs: f_X) and the cumulative distribution functions (CDFs:F_X) of the two channel gains h_1, g_i is Gamma distributions. Hence $|h_1|^2$, $|g_i|^2$ is expressed as Nakagami m fading by

$$F_X(x) = 1 - \frac{1}{\Gamma(m_i)}\Gamma\left(m_i, \frac{m_i x}{(1-\rho)\Omega_A}\right). \tag{11}$$

$$f_X(x) = \left(\frac{m_i}{(1-\rho)\Omega_A}\right)^{m_i} \frac{x^{m_i-1}}{\Gamma(m_i)} \exp\left(-\frac{m_i x}{(1-\rho)\Omega_A}\right). \tag{12}$$

Replace (6) and (8) into (9) and (10), we obtained OPD_1 and OPD_2. The detail is as follows

By using SINR expressed in (6), (8), we can rewritten the outage probability of (9) into (13). Note that self-interference channel is Gamma distribution with parameters m.

$$\begin{aligned}\mathrm{OPD}_1 &\simeq 1 - \Pr\left(\frac{a_1}{a_2 + \phi Z} > \gamma_{\mathrm{th}_1}, \frac{a_1 \phi XY}{a_2 \phi XY + 1} > \gamma_{\mathrm{th}_1}\right) \\ &= 1 - \left[1 - \exp\left(-\frac{\varpi_1}{\kappa\Omega_{LI}}\right)\right] \underbrace{\int_0^\infty \Pr\left(X > \frac{\psi}{y}\right) f_Y(y) dy}_{I_1}.\end{aligned} \tag{13}$$

where $\varpi_1 = \frac{a_1}{\phi\gamma_{\mathrm{th}_1}} - \frac{a_2}{\phi}$, $\psi = \frac{\gamma_{\mathrm{th}_1}}{\phi P_S(a_1 - a_2\gamma_{\mathrm{th}_1})}$. Based on the CDF and PDF in (11) and (12) we have

$$I_1 = 1 - \int_0^\infty \left[1 - \frac{1}{\Gamma(m_1)}\Gamma\left(m_1, \frac{m_1\psi}{y(1-\rho)\Omega_{\mathrm{SR}}}\right)\right] \left(\frac{m_2}{(1-\rho)\Omega_{\mathrm{RD}_1}}\right)^{m_2} \frac{y^{m_2-1}}{\Gamma(m_2)} \exp\left(-\frac{m_2 y}{(1-\rho)\Omega_{\mathrm{RD}_1}}\right). \tag{14}$$

Thanks to the help of [16, Eq. (8.352.4)] and [16, Eq. (3.471.9)], after some manipulations of (14), we obtain the closed-form of outage probability of D_1 as

$$\begin{aligned}\mathrm{OPD}_1 = 1 &- \left[1 - \exp\left(-\frac{\varpi_1}{\kappa\Omega_{LI}}\right)\right] \sum_{k=0}^{m_1-1} \frac{1}{k!} \left(\frac{m_1\psi}{(1-\rho)\Omega_{\mathrm{SR}}}\right)^k \left(\frac{m_2\psi}{(1-\rho)\Omega_{\mathrm{RD}_1}}\right)^{m_2} \\ &\times \left(\frac{m_1\psi\Omega_{\mathrm{RD}_1}}{\Omega_{\mathrm{SR}} m_2}\right)^{\frac{m_2-k}{2}} \frac{2}{\Gamma(m_2)} K_{m_2-k}\left(2\sqrt{\frac{m_1 m_2 \psi}{(1-\rho)^2 \Omega_{\mathrm{SR}}\Omega_{\mathrm{RD}_1}}}\right),\end{aligned} \tag{15}$$

where $K_n(\cdot)$ is the first-order modified Bessel function of the second kind [16].

To derive the outage probability of the D_2, we replace (6), (8) into (10), and obtain (16).

$$\mathrm{OPD}_2 = 1 - \Pr\left(\begin{array}{l} |h_{LI}|^2 < \min\left\{\frac{a_1}{\phi\gamma_{\mathrm{th}_1}} - \frac{a_2}{\phi}, \frac{a_1 P_S |h_1|^2 - \gamma_{\mathrm{th}_2}}{\gamma_{\mathrm{th}_2}\phi P_S |h_1|^2}\right\} \\ |g_2|^2 > \max\left\{\frac{\gamma_{\mathrm{th}_1}}{\phi P_S |h_1|^2 (a_1 - a_2\gamma_{\mathrm{th}_1})}, \frac{\gamma_{\mathrm{th}_2}}{a_2\phi P_S |h_1|^2}\right\} \end{array}\right). \tag{16}$$

The probability in (16) can be rewritten as (17) and it is recognized that the outage always occurs if $a_1 \le a_2\gamma_{\mathrm{th}_1}$ or $a_1 \le a_2\gamma_{\mathrm{th}_2}$. Hence, we need to allocate more power to D_1, i.e., $a_1 > a_2\gamma_{\mathrm{th}_1}$ and $a_1 > a_2\gamma_{\mathrm{th}_2}$.

$$\begin{aligned} \mathrm{OPD}_2 = 1 &- \underbrace{\Pr\left(\begin{array}{l} Z < \frac{a_1}{\phi\gamma_{\mathrm{th}_1}} - \frac{a_2}{\phi}, \frac{a_1}{\phi\gamma_{\mathrm{th}_1}} - \frac{a_2}{\phi} < \frac{a_2 P_S X - \gamma_{\mathrm{th}_2}}{\gamma_{\mathrm{th}_1}\phi P_S X} \\ W > \frac{\gamma_{\mathrm{th}_2}}{\phi P_S X (a_1 - a_2\gamma_{\mathrm{th}_2})}, \frac{\gamma_{\mathrm{th}_2}}{\phi P_S X (a_1 - a_2\gamma_{\mathrm{th}_2})} > \frac{\gamma_{\mathrm{th}_2}}{a_2\phi P_S X} \end{array}\right)}_{Q_1} \\ &+ \underbrace{\Pr\left(\begin{array}{l} Z < \frac{a_2 P_S X - \gamma_{\mathrm{th}_1}}{\gamma_{\mathrm{th}_1}\phi P_S X}, \frac{a_2 P_S X - \gamma_{\mathrm{th}_1}}{\gamma_{\mathrm{th}_1}\phi P_S X} < \frac{a_1}{\phi\gamma_{\mathrm{th}_1}} - \frac{a_2}{\phi} \\ W > \frac{\gamma_{\mathrm{th}_2}}{a_2\phi P_S X}, \frac{\gamma_{\mathrm{th}_2}}{a_2\phi P_S X} > \frac{\gamma_{\mathrm{th}_2}}{\phi P_S X (a_1 - a_2\gamma_{\mathrm{th}_2})} \end{array}\right)}_{Q_2}. \end{aligned} \tag{17}$$

To calculate OPD_2, we need calculate Q_1 and Q_2, respectively. The first part in (17) can be represented as in (18).

$$Q_1 = \Pr\left(\begin{array}{l} Z < \frac{a_1}{\phi\gamma_{\mathrm{th}_1}} - \frac{a_2}{\phi}, X > \frac{\gamma_{\mathrm{th}_1}}{P_S(a_1 - a_2(1+\gamma_{\mathrm{th}_1}))}, \\ W > \frac{\gamma_{\mathrm{th}_2}}{\phi P_S (a_1 - a_2\gamma_{\mathrm{th}_1})}, a_1 > a_2(1+\gamma_{\mathrm{th}_1}) \end{array}\right). \tag{18}$$

In order to satisfy condition in (18) meaning all factors are positive, the power allocation coefficient a_1 should be $a_1 \ge \frac{1+\gamma_{\mathrm{th}_1}}{2+\gamma_{\mathrm{th}_1}}$ and $a_1 > \frac{\gamma_{\mathrm{th}_1}}{1+\gamma_{\mathrm{th}_1}}$.

Note that $a_1 = 1 - a_2$ and because of $\frac{1+\gamma_{\mathrm{th}_1}}{2+\gamma_{\mathrm{th}_1}} > \frac{\gamma_{\mathrm{th}_1}}{1+\gamma_{\mathrm{th}_1}}$, the final condition of a_1 is decided as $a_1 \ge \frac{1+\gamma_{\mathrm{th}_1}}{2+\gamma_{\mathrm{th}_1}}$.

From (18), we have $Q_1 = \Pr(Z < \varpi_2) \int_{\frac{\gamma_{\mathrm{th}_1}}{P_S\delta}}^{\infty} \left[1 - F_W\left(\frac{\Phi}{x}\right)\right] f_X(x)dx$, where $\Phi = \frac{\gamma_{\mathrm{th}_1}}{P_S(a_1 - a_2(1+\gamma_{\mathrm{th}_1}))}$, $\varpi_2 = \frac{a_1}{\phi\gamma_{\mathrm{th}_1}} - \frac{a_2}{\phi}$ and $\delta = a_1 - a_2(1+\gamma_{\mathrm{th}_2})$. The power transmit of the source is assumed to be lager enough. Hence, we can be approximated as follows.

$$Q_1 \approx \left[1 - \exp\left(-\frac{\varpi_2}{\kappa\Omega_{LI}}\right)\right] \underbrace{\int_0^{\infty} \left[1 - F_W\left(\frac{\Phi}{x}\right)\right] f_X(x)dx}_{I_2}. \tag{19}$$

From (11) and (12), thanks to the help of [16, Eq. (3.471.9)], the closed-form of I_2 is given as in (20)

$$I_2 \approx \sum_{q=0}^{m_1-1} \frac{2}{q!\Gamma(m_1)} \left(\frac{m_1\Phi}{(1-\rho)\Omega_{\mathrm{SR}}}\right)^{m_1} \left(\frac{m_3\Phi\Omega_{\mathrm{SR}}}{(1-\rho)\Omega_{\mathrm{RD}_2}m_1}\right)^{\frac{m_1-q}{2}} \left(\frac{m_3\Phi}{(1-\rho)\Omega_{\mathrm{RD}_2}}\right)^{q} K_{m_1-q}\left(\sqrt{\frac{4m_1m_3\Phi}{(1-\rho)^2\Omega_{\mathrm{SR}}\Omega_{\mathrm{RD}_2}}}\right). \quad (20)$$

Due to the condition of $a_1 \geq \frac{1+\gamma_{\mathrm{th}_1}}{2+\gamma_{\mathrm{th}_1}}$ the second part in (17) becomes zero.

$$Q_2 = \Pr\left(\begin{array}{c} Z < \frac{a_1}{\phi\gamma_{\mathrm{th}_1}} - \frac{a_2}{\phi}, X \leq \frac{\gamma_{\mathrm{th}_1}}{P_{\mathrm{S}}(a_1 - a_2(1+\gamma_{\mathrm{th}_1}))}, \\ W > \frac{\gamma_{\mathrm{th}_2}}{\phi P_{\mathrm{S}} X}, a_1 \leq a_2(1+\gamma_{\mathrm{th}_1}) \end{array}\right) = 0. \quad (21)$$

Replace Q_1 and Q_2 into (17), we have the closed-form OP of the D_2.

$$\begin{aligned} \mathrm{OPD}_2 = 1 - \left[1 - \exp\left(-\frac{\varpi_2}{\kappa\Omega_{LI}}\right)\right] \sum_{q=0}^{m_1-1} \frac{1}{q!} \left(\frac{m_1\Phi}{(1-\rho)\Omega_{\mathrm{SR}}}\right)^{m_1} \left(\frac{m_3\Phi}{(1-\rho)\Omega_{\mathrm{RD}_2}}\right)^{q} \\ \times \left(\frac{m_1\Phi\Omega_{\mathrm{SR}}}{\Omega_{\mathrm{RD}_2}m_3}\right)^{\frac{m_1-q}{2}} \frac{2}{\Gamma(m_3)} K_{m_1-q}\left(2\sqrt{\frac{m_1m_3\Phi}{(1-\rho)^2\Omega_{\mathrm{SR}}\Omega_{\mathrm{RD}_2}}}\right). \end{aligned} \quad (22)$$

4 Simulation Result

In this section, the numerical results are provided to illustrate the impact of the estimation error and strength of self-interference at the relay node on the performance of SWIPT-NOMA system in terms of the outage performance.

The parameters of the system are as follows. Since the D_2 is closer to the relay nodes than D_1, without loss of generality, we let $\mathbb{E}\{|h_{\mathrm{SR}}|^2\} = \Omega_{\mathrm{SR}} = \mathbb{E}\{|g_{\mathrm{RD}_2}|^2\} = \Omega_{\mathrm{RD}_2} = 1$ and $\mathbb{E}\{|g_{\mathrm{RD}_1}|^2\} = \Omega_{\mathrm{RD}_1} = 0.75$. Hence, we need to allocate more power to D_1 than D_2 to ensure the fairness of users. Moreover, the target transmission rate of D_1 and D_2 is assumed to be the same, i.e., $r_1 = r_2 = 0.5[b/s/Hz]$. The transmit power is allocated following the ratio: $\frac{a_1}{a_2} = \frac{\Omega_{\mathrm{RD}_2}}{\Omega_{\mathrm{RD}_1} + \Omega_{\mathrm{RD}_2}}$. The energy harvesting fraction $\alpha = 0.33$, the energy conversion efficiency $\eta = 0.85$ and the estimated channel coefficients $\rho_{\mathrm{SR}} = \rho_{\mathrm{RD}_1} = \rho_{\mathrm{RD}_2} = \rho$.

In Fig. 2, we investigate the outage probability of the D_1 and D_2 with fixed power allocations, i.e., $\frac{a_1}{a_2} = \frac{\Omega_{\mathrm{RD}_2}}{\Omega_{\mathrm{RD}_1} + \Omega_{\mathrm{RD}_2}}$. In these figures, we can see that the theoretical analysis matches for the simulation results, especially at the mean and high SNR regions. This is reasonable, we have approximated the outage probabilities under the condition of high SNR. However, this result is acceptable for all regions of SNR. On the other hand, in these results we also investigated the value of the fading severity m_i impact on the outage performance. The distribution of the channels is considered following Nakagami-m and the Rayleigh fading can be viewed as a special case by setting $m_i = 1$. By changing the value of m, the proposed model channel is adopted to investigate the practical application

of EH NOMA in 5G networks, such as in IoT, wireless sensor networks and cellular communication systems. Furthermore, as shown in Fig. 2a, the performance of the D_2 is better than D_1, although the power allocate for D_1 is larger than that of D_2. The reason is the D_2 is close to R in comparison with D_1, i.e., the channel gain of the D_2 is higher than D_1. Moreover, due to the impact of self-interference at the relay node, the outage probability saturates when the average SNRs increase.

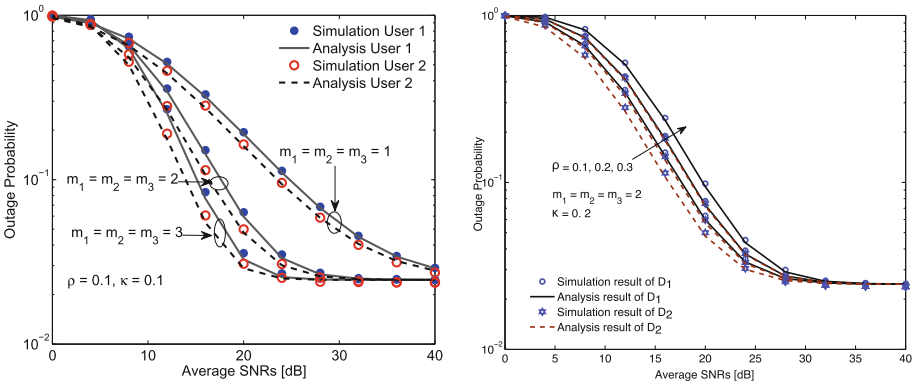

(a) Impact of fading severity on the outage probability

(b) Impact of the channel estimation error on the OP.

Fig. 2. Outage probability of D_1 and D_2

In Fig. 2b, we investigated the impact of the correlation coefficient of the estimated and practical channels on the outage performance. In this figure, we observe that the outage probability decreases according to the transmit power of the source and converges on a certain value when transmitting power is large enough. The reason is, the transmit power of relay increase is directly proportional with the transmit power of the source. Therefore, when the transmit power of the source increases, the SINR of relay increases. However, when the transmit power of the source is large enough, the transmit power of relay is also large and much higher than the noise. Hence, the term of noise is negligibility. As a result, the SINR of relay is constant because of self-interference term.

Figure 3a depicts the effect of the power allocation coefficient on the outage probability. It should be noted that we only derived the coefficient for minimum the outage probability of the D_2 under condition of fairness in outage performance between D_1 and D_2. This means that, the power allocation coefficient for D_1 is not too large to ensure the decoding symbol x_2 of D_2 is successful. As shown in Fig. 3a, for different severe fading m_i the different minimal values of the outage probability are exhibited.

Figure 3b demonstrate OP versus average SNR in dB. Firstly, we see that difference energy harvesting duration time, leading to the fact that difference system performance. At the low SNR we can increase α to improve OP, but at the high SNR that is saturated.

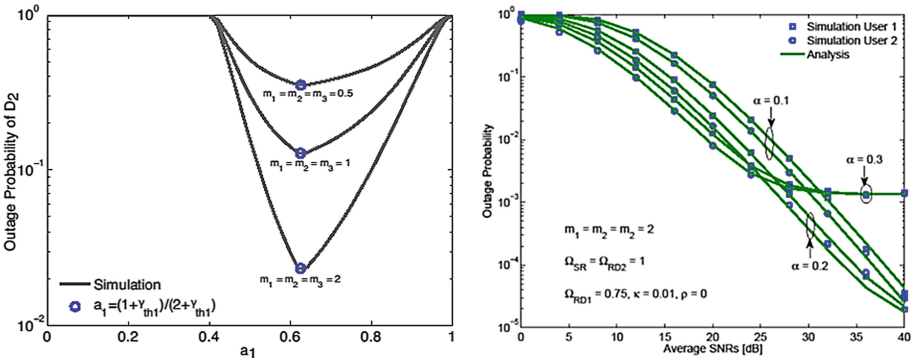

(a) Impact of the power allocation coefficient for minimum the OP.

(b) Impact of the energy harvesting duration time on OP

Fig. 3. Outage probability

5 Conclusion

In this paper, we propose a NOMA cooperative full-duplex relay network. In addition, the relay node harvests the energy from the source using the time-switching mechanism. We focus on deriving the outage probability of the system over Nakagami m fading channels which was not considered in previous works. In addition, we consider the impact of channel estimation error on the performance of system. Moreover, we derived the optimal power allocation coefficient in the sense of minimal outage probability while keeping the fairness in outage performance of two end users. The theoretical closed-form expressions that we have derived in this paper are verified by the Monte-Carlo simulations.

In this paper, we have considered a system which consists of one source, one relay and two users, the more general system will be considered in our future works.

References

1. Wang, Y., Ren, B., Sun, S., Kang, S., Yue, X.: Analysis of non-orthogonal multiple access for 5G. China Commun. **13**(Supplement 2), 52–66 (2016)
2. Dai, L., Wang, B., Yuan, Y., Han, S., Chih-Lin, I., Wang, Z.: Non-orthogonal multiple access for 5G: solutions, challenges, opportunities, and future research trends. IEEE Commun. Mag. **53**(9), 74–81 (2015)
3. Luo, S., Teh, K.C.: Adaptive transmission for cooperative NOMA system with Buffer-Aided Relaying. IEEE Commun. Lett., January 2017
4. Kader, M.F., Shahab, M.B., Shin, S.-Y.: Exploiting non-orthogonal multiple access in cooperative relay sharing. IEEE Commun. Lett., January 2017
5. Du, C., Chen, X., Lei, L.: Energy-efficient optimization for secrecywireless information and power transfer in massive MIMO relaying systems. IET Commun. **11**(1), 10–16 (2017)
6. Chen, Y.: Energy-harvesting AF relaying in the presence of interference and Nakagami-fading. IEEE Trans. Commun. **15**(2), 1008–1017 (2016)

7. Boshkovska, E., Ng, D.W.K., Zlatanov, N., Schober, R.: Practical non-linear energy harvesting model and resource allocation for SWIPT systems. IEEE Commun. Lett. **19**(12), 2082–2085 (2015)
8. Varshney, L.R.: Transporting information and energy simultaneously. In: IEEE Transactions on Information Theory, pp. 1612–1616, August 2008
9. Liu, Y., Ding, Z., Elkashlan, M., Poor, H.V.: Cooperative non-orthogonal multiple access with simultaneous wireless information and power transfer. IEEE J. Sel. Areas Commun. **34**(4), 938–953 (2016)
10. Han, W., Ge, J., Men, J.: Performance analysis for NOMA energy harvesting relaying networks with transmit antenna selection and maximal-ratio combining over Nakagami-m fading. IET Commun. **10**(18), 2687–2693 (2016)
11. Yang, Z., Ding, Z., Fan, P., Al-Dhahir, N.: The impact of power allocation on cooperative non-orthogonal multiple access networks with SWIPT. IEEE Trans. Wireless Commun. **16**(7), 4332–4343 (2017)
12. Michalopoulos, D.S., Suraweera, H.A., Schober, R.: Relay selection for simultaneous information transmission and wireless energy transfer: a tradeoff perspective. IEEE J. Sel. Areas Commun. **33**(8), 1578–1594 (2015)
13. Chen, Y., Wang, L., Jiao, B.: Cooperative multicast non-orthogonal multiple access in cognitive radio. In: International Conference on Communications (ICC), pp. 1–6. IEEE, May 2017
14. Lee, K., Hong, J.-P.: Energy-efficient resource allocation for simultaneous information and energy transfer with imperfect channel estimation. IEEE Trans. Veh. Commun. **65**(4), 2775–2780 (2016)
15. Suraweera, H.A., Smith, P.J., Shafi, M.: Capacity limits and performance analysis of cognitive radio with imperfect channel knowledge. IEEE Trans. Veh. Technol. **59**(4), 1811–1822 (2010)
16. Zwillinger, D.: Table of integrals, series, and products. Elsevier, (2007)